

Surface structural investigations on (1 0 0) and (1 1 0) faces of flux-grown lanthanum borate crystals

P. N. KOTRU, ANIMA JAIN, ASHOK K. RAZDAN,
Department of Physics, University of Jammu, Jammu Tawi 180 001, India

B. M. WANKLYN
Clarendon Laboratory, Department of Physics, University of Oxford, Oxford, UK

Results of topographical studies carried out on (1 0 0) and (1 1 0) faces of lanthanum borate crystals grown from the $\text{PbO-B}_2\text{O}_3$ flux system are illustrated and discussed. The habit faces display the formation of cavities, microcrystals, elliptical etch pits, elliptical hillocks, circular hillocks and irregular structures. Also described are a various number of elevated structures identified as impurity phases. Energy dispersive X-ray (EDAX) studies have confirmed that these impurity phases in the growth of lanthanum borate (LaBO_3) crystals are enriched by lead (Pb). The habit faces also exhibit some elevated regions which are reported to be more imperfect in comparison with others. It is inferred that independent growth on the habit faces has taken place during the last stage of crystal growth by a two-dimensional nucleation mechanism.

1. Introduction

Surface structural studies allow us to understand the history, mechanism and process of crystal growth and its dissolution. In addition, one can determine the macromorphology (crystal habit) and micromorphology (microtopography of crystal faces). Because the crystal grows and develops through faces, every phenomenon pertaining to growth and dissolution mechanisms is perfectly registered on the surfaces. The habit faces of a crystal are the ends of growth and hence they yield more information about the conditions and mechanism of growth in the final stages. However, it is not always difficult to work out the entire process of crystal growth and/or dissolution mechanisms through surface structural studies. Hence one can safely say that solutions of problems associated with growth or dissolution should lie in the surface itself. One can also determine the relation between crystalline perfection and different parameters of growth; the study is important especially in the case of crystals grown in sealed systems, where it is difficult to watch the growing crystals *in situ*. In such cases, there is no alternative to the employment of indirect means for furnishing information regarding the growth mechanism and dissolution process of the grown crystals. The flux growth of LaBO_3 involves very high temperatures and the growing system is sealed. Microtopography, therefore, is a very appropriate means of yielding information pertaining to the growth mechanism. Surface structural studies have provided important information in the case of many crystals [1-13].

The appearance of RBO_3 as an unwanted phase during the flux growth of other rare earth compounds

from $\text{PbO-B}_2\text{O}_3$ [14] and from $\text{PbO-PbF}_2\text{-B}_2\text{O}_3$ [15] fluxes was reported in 1965. However, their growth as single crystals was not reported until 1973. Wanklyn [16] reported the flux growth of RBO_3 ($\text{R} = \text{La, Pr, Nd, Er and Lu}$) single crystals. The experiments of Wanklyn [16] yielded crystals of LaBO_3 , mainly as transparent platelets. However, Kotru and Wanklyn [17] reported the growth of LaBO_3 as single crystals of varied morphologies. They grew as (i) platelets with the major faces as (1 0 0) and long direction along the *c*-axis, (ii) tabular prisms with (1 0 0) and (1 1 0) faces, (iii) rods and (iv) approximately equidimensional crystals as mentioned in the literature [17]. The rare earth borates, RBO_3 , fall into three groups according to their crystal structure, each being structurally related to one of three forms of calcite. LaBO_3 crystal has orthorhombic structure of aragonite and is pseudo-hexagonal, with the pseudo-hexagonal *c*-axis parallel to the orthorhombic *b*-axis [19-21]. Kotru and Wanklyn [17] performed various experiments according to a proposed model which predicted the starting compositions for the flux growth of LaBO_3 crystals with one refractory (La_2O_3) and one relatively low melting component (B_2O_3) from fluxed melts [22].

In this paper we report the results of surface structures on (1 0 0) and (1 1 0) faces of flux-grown LaBO_3 crystals using optical and scanning electron microscopy and energy dispersive analysis of X-rays (EDAX) techniques for the identification of impurity phases. It may be noted that no work has been reported on the surface topography of these crystals.

2. Experimental techniques

Growth of LaBO_3 as single crystals have been reported by Kotru and Wanklyn [17]. Experiments were performed in the system $\text{La}_2\text{O}_3\text{-PbO-B}_2\text{O}_3$ and the proportion of La_2O_3 was varied. The starting composition was pressed into a platinum crucible of appreciable volume and then heated to a maximum temperature of 1260°C . The crucible was soaked for 15 h in a specially designed furnace and then cooled at the rate of 3°C h^{-1} to 700°C . The crystals were mechanically separated from the flux [18], but because they dissolve even in dilute acid, could not be soaked in acid in the usual way.

The crystals were thoroughly cleaned and then the desired surfaces coated with thin films of silver (in most cases) in a vacuum coating plant (Hind Hivac-12A4) to enhance the reflectivity of the crystal surfaces. Some typical structures on (100) and (110) faces of LaBO_3 crystals were examined by using the metallurgical microscope neophot-2 (Carl Zeiss, Germany) and scanning electron microscope, S4-10 (Cambridge Stereo Scan). An energy dispersive spectrometer (KcVx) attached to the scanning unit was used for elemental analysis.

3. Results and discussion

Flux growth yields crystals with habit faces and are therefore very suitable for microtopographical investigations. During the present study, crystals grown in different batches using varying starting compositions were used.

3.1. LaBO_3 crystals (batch A)

This batch of crystals was grown from the following compositions 5.28 g PbO_2 , 33.6 g PbO , 1.92 g B_2O_3 , 3.168 g La_2O_3 .

3.1.1. Impurity phases

During flux growth, some impurities become precipitated as secondary phases. Kotru *et al.* have reported precipitation of secondary phases like magnetoplumbite ($\text{PbO} \cdot 6\text{Fe}_2\text{O}_3$), RBO_3 and ROF during the flux growth of ErFeO_3 [23, 24], HoFeO_3 [25] and DyFeO_3 [26] from the $\text{PbO-PbF}_2\text{-B}_2\text{O}_3$ flux system. The secondary phases help stimulation of localized growth and thus adversely affect the perfection of the growing crystal [23]. Covering the process of impurity phases by advancing growth fronts leads to formation of microdiscs on the crystal surfaces [25]. It is reported that Pb_2CrO_5 is precipitated as a secondary phase during the flux growth of YbCrO_3 [27, 28] and LaCrO_3 [20]. Fig. 1 is a scanning electron micrograph of a (100) face of an LaBO_3 crystal. One observes features like linear strips and irregular shaped elevations.

Fig. 2a shows one of the regions of Fig. 1 at a higher magnification. The region contains linear strips and the irregular elevations. An X-ray mapping image of the region of Fig. 2a reveals detection of $\text{PbM}\alpha$ radiations (see Fig. 2b). It shows the distribution of lead over the crystal surface. Fig. 2c is the X-ray mapping image when the instrument is set for the detection of $\text{LaL}\alpha$ radiation. The distribution of lanthanum over the surface of Fig. 2a is indicated in this figure.

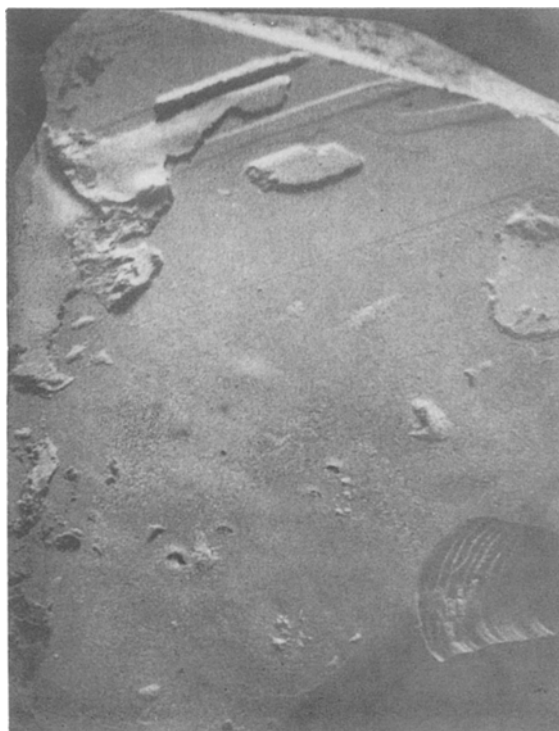


Figure 1 A scanning electron micrograph showing a face with irregular islands and linear strips ($\times 100$).

From Figs 2a to c, the following deductions can be made.

1. The irregular elevations and thick linear strips seen in Fig. 2a are rich in lead (see Fig. 2b) and practically devoid of lanthanum (see Fig. 2c). The thin linear strips with a plane surface area of the same material as the general surface (i.e. LaBO_3). The material containing lead is probably residual flux.

2. The general plane surface of Fig. 2a has a nearly uniform distribution of lanthanum (see Fig. 2c).

The above observations confirm the formation of thick linear strips and irregular elevations to be the result of precipitation of some secondary phase which is rich in lead. The secondary phase appears to have been precipitated almost at the end of LaBO_3 growth. There are no indications of any modifications of growth fronts by either the linear strips or the irregular elevations. Because of the precipitation of such secondary phases, the surfaces are rendered imperfect.

The above results are further supported by observations from Figs 3 and 4. Fig. 3 is a scanning electron micrograph showing one of the regions of Fig. 1 at a higher magnification. Here also one observes irregularly shaped elevations, big (in the central region) and small, scattered all over the surface. At first sight they do not appear to be of the same phase as the general surface (LaBO_3) and could possibly be deposition of secondary phases. Fig. 4 is an EDAX spectrum recorded over the central region (encircled) of Fig. 3. The spectrum shows peaks due to $\text{PbM}\alpha$ besides those due to La. EDAX spectra recorded on the general surface exhibit peaks due to lanthanum only. From this result it is clear that the impurity phases rich in lead are precipitated in the flux growth of LaBO_3 from the $\text{PbO-B}_2\text{O}_3$ flux system. Fig. 5 is a scanning electron micrograph showing a similar example of deposition of a secondary phase rich in lead. A region of

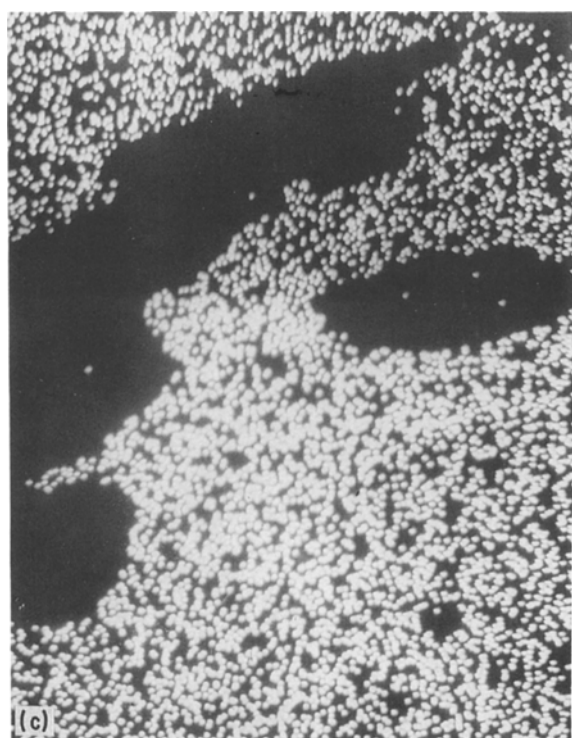
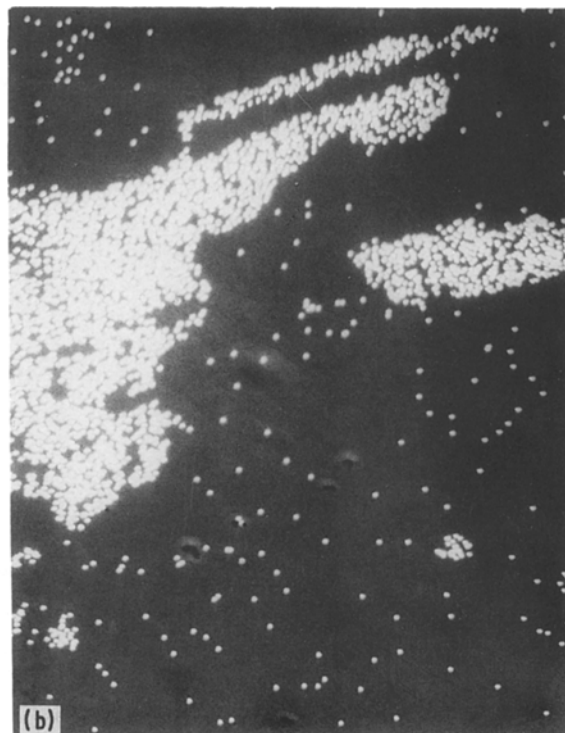


Figure 2 (a) A scanning electron micrograph showing a region of Fig. 1 at a higher magnification. It shows the region containing irregular elevations and linear strips ($\times 128$). (b) X-ray mapping image of the surface of (a) revealing detection of $PbM\alpha$ radiation, indicating the distribution of lead over the surface of (a) ($\times 128$). (c) X-ray mapping image showing detection of $LaL\alpha$ radiation indicating distribution of lanthanum over the surface of (a) ($\times 128$).

Fig. 5 containing the deposition is shown at a higher magnification in Fig. 6. The deposition is irregularly distributed over the surface.

3.1.2. Cavities and microcrystals

Fig. 7 is an optical micrograph taken on the (110) face of an $LaBO_3$ crystal. It shows irregularly shaped cavities. The cavities seem to have formed as a result of impurities which were blown off the surface. The cavities are shown at a higher magnification in Fig. 8. Fig. 9 is an optical micrograph showing microcrystals crowded together on the surface of Fig. 7. The microcrystals seem to have formed almost at the end of bulk growth of $LaBO_3$.



Figure 3 A scanning electron micrograph showing one of the regions of Fig. 1 at a higher magnification. The region shows irregular shaped elevations ($\times 1280$).

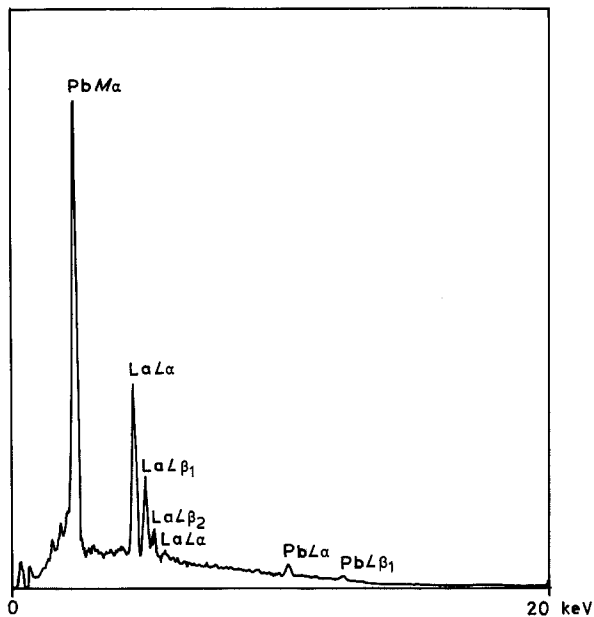


Figure 4 An EDAX curve recorded over the circled region of Fig. 3 indicating peaks due to lanthanum and lead.

3.1.3. Elliptical etch pits

Fig. 10 is an optical micrograph showing elliptical etch pits on a (100) face of a tabular type of LaBO_3 crystal. The pits are oriented; their longer diagonals being parallel to the edges of intersection between (100) and (110) faces. It is conjectured that the etch pits may have developed at the end of crystal growth as a result of dissolution by the flux system.

3.2. LaBO_3 crystal (batch B)

This batch of crystals was grown from the following composition: 5.28 g PbO_2 , 33.6 g PbO , 1.9 g B_2O_3 , 3.456 g La_2O_3 .

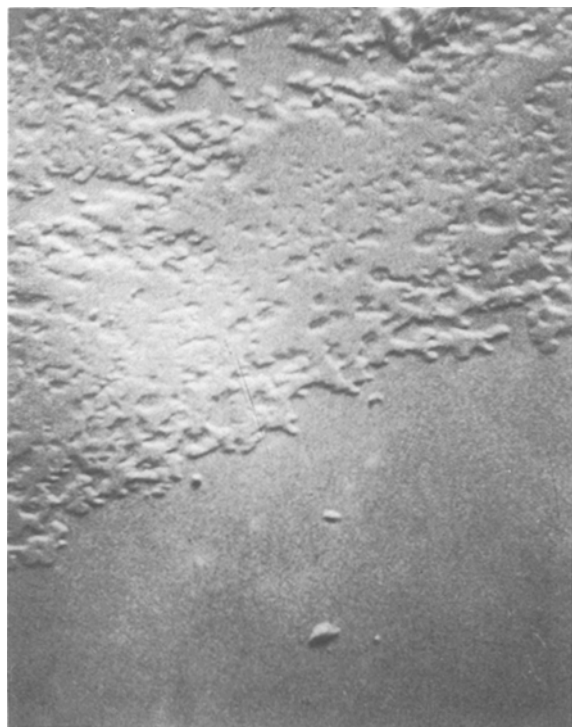


Figure 5 A scanning electron micrograph showing thin deposition of impurity phases rich in lead ($\times 640$).

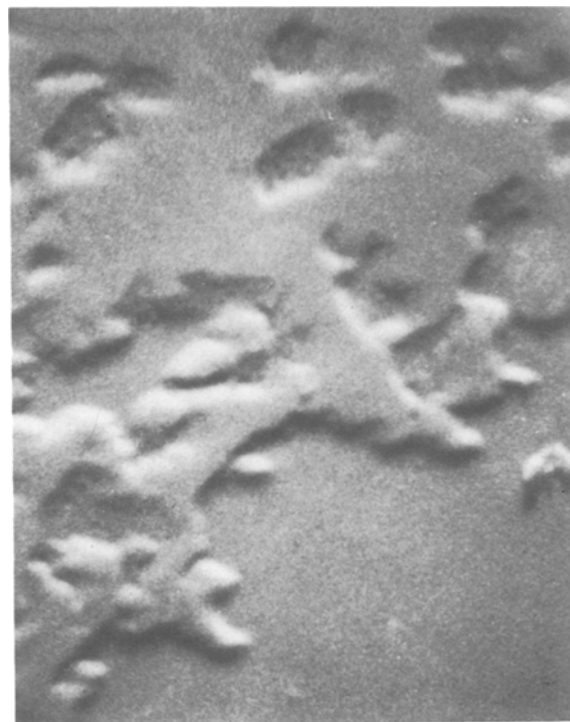


Figure 6 A region of Fig. 5 at a higher magnification revealing irregular deposition of the impurity phase ($\times 2560$).

3.2.1. Elliptical hillocks

Fig. 11 is an optical micrograph showing elliptical hillocks on a (100) face of an LaBO_3 crystal. Here also, the longer diagonals of these hillocks are parallel to the edges of the intersection between (100) and (110) faces; the hillocks being oriented but of varying sizes. Fig. 12 shows a region of Fig. 11 after etching the crystal in 90% HNO_3 at 35°C for 2 h. Most of the smaller hillocks are washed off on etching. However, the larger ones are still seen on the surface. It is observed that the summit of none of the hillocks is preferentially etched. Its formation, therefore, is not likely to be due to screw dislocations. However, it is seen that the density of etch pits is much higher over the hillock than elsewhere on the general surface. To illustrate this here, the circled region of Fig. 12 is shown at a higher magnification in Fig. 13, where a higher density of etch pits over the hillock is found.

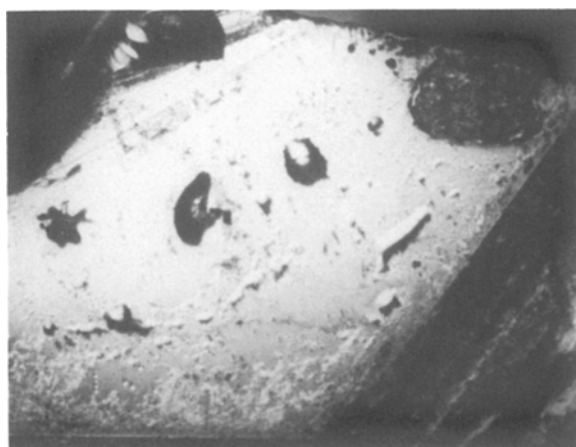


Figure 7 Optical micrograph of a habit face showing irregular shaped cavities ($\times 40$).

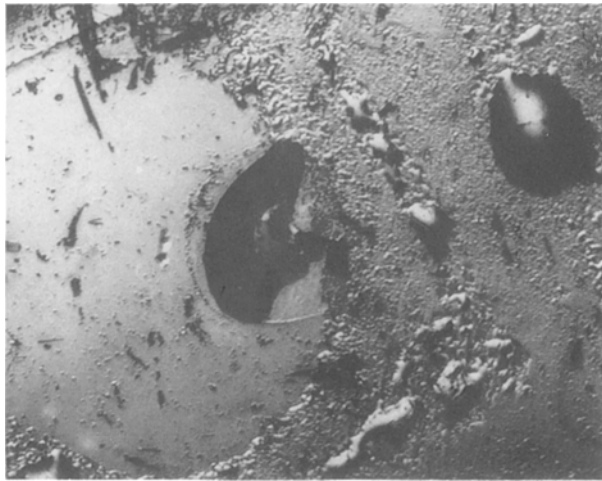


Figure 8 A region of Fig. 7 at higher magnification showing the region containing irregular cavities ($\times 101$).

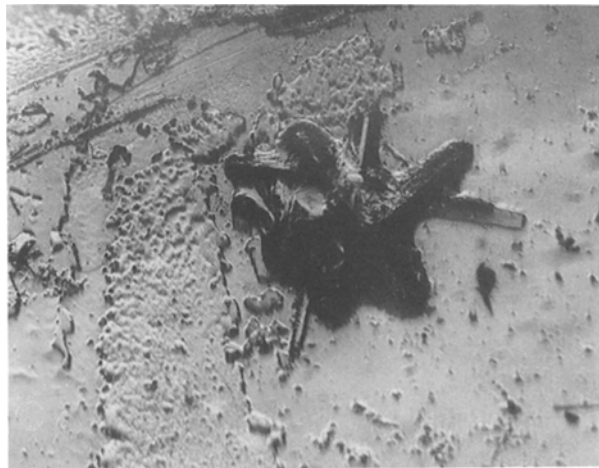


Figure 9 An optical micrograph showing microcrystals attached to the host face of Fig. 7 ($\times 160$).

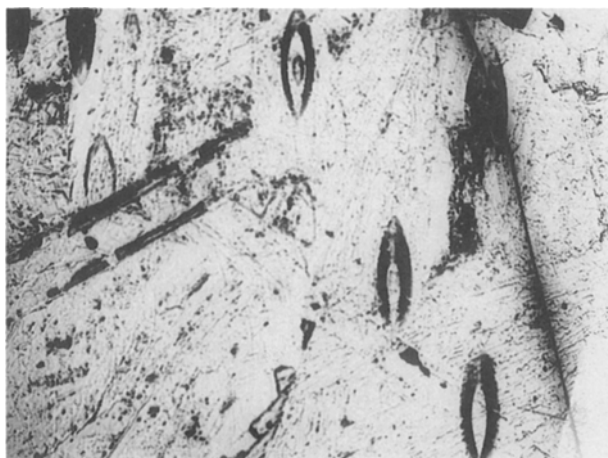


Figure 10 An optical micrograph showing elliptical etch pits on a (100) face of a tabular type of LaBO_3 crystal. The longer side of the micrograph are parallel to the edges of intersections between (100) and (110) ($\times 40$).

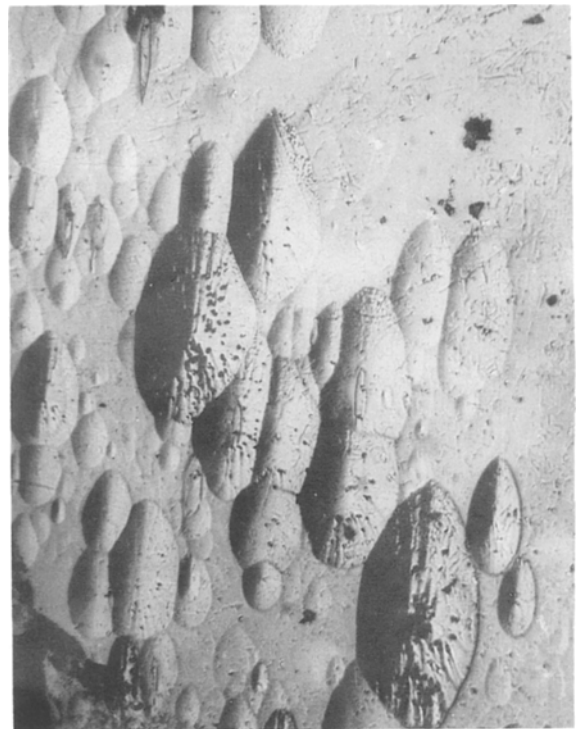


Figure 11 An optical micrograph showing elliptical hillocks on a (110) face ($\times 78$).

The result indicates the region of the hillock to be more imperfect than the (100) surface in general.

Some faces exhibited a very high density of elliptical flat-topped hillocks. Here also, the hillocks are strictly oriented as can be seen from the photograph in Fig. 14. A region of Fig. 14 is shown at a higher magnification in Fig. 15. A flat-topped hillock within the marked region of Fig. 15 is shown in Fig. 16. The topography of the hillock is clearly seen. The hillock has an egg-shaped base with a flat top. It is terraced, one of the

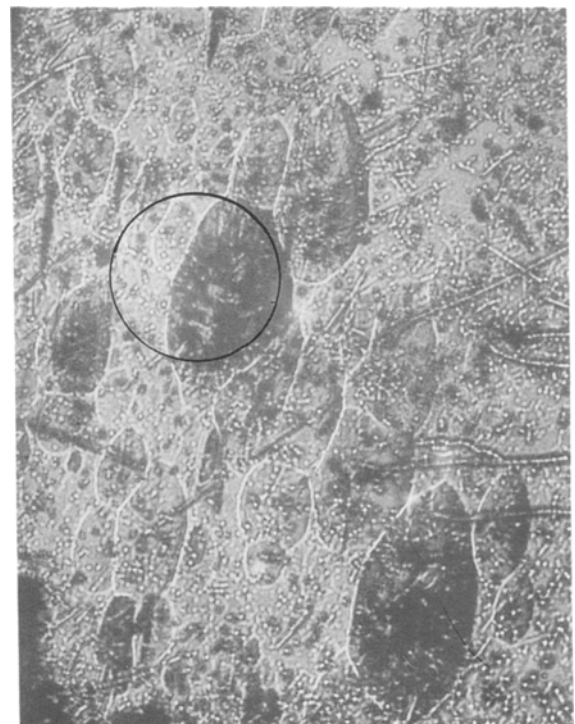


Figure 12 The corresponding region of Fig. 11 after 2h of etching in 90% HNO_3 at 35°C ($\times 78$).

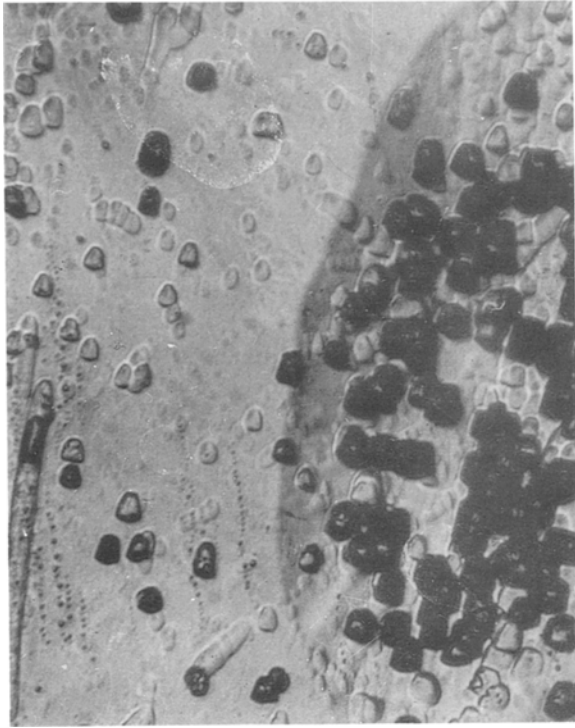


Figure 13 The circled region of Fig. 12 at a higher magnification revealing a higher density of etch pits in the region of a hillock ($\times 1000$).

terraces being steeper. It is also interesting to note that some irregular cavities have developed on top of the hillocks. It seems that elevations (flat-topped hillocks) are formed after the cessation of crystal growth as there is no evidence of modification of growth fronts. The formation of irregular cavities (Figs 14 to 16) may be attributed as a result of either the detachment of impurities from the surface or the heavy dissolution by the flux system.



Figure 14 An optical micrograph showing elliptical shaped flat-topped hillocks ($\times 200$).

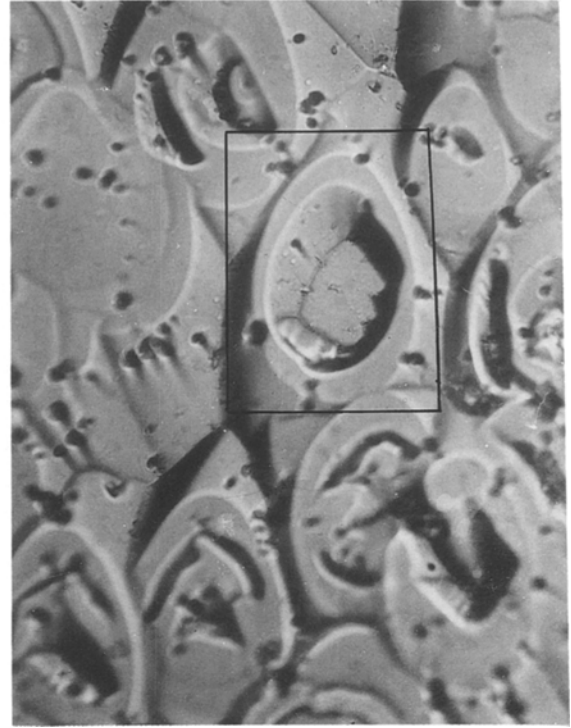


Figure 15 A region of Fig. 14 at a higher magnification showing flat-topped hillocks ($\times 400$).

3.2.2. Circular hillocks and irregular structures

Fig. 17 is an optical micrograph showing circular hillocks observed on the (100) face of LaBO_3 of this batch. The hillocks are of varying sizes. Most are flat topped but a very few of them do have a pointed summit.

Some faces exhibited irregular deposition of LaBO_3 on their general surface. Fig. 18 is an optical micrograph illustrating one such case. It seems that this



Figure 16 A hillock within the marked region of Fig. 15 revealing its structure ($\times 1000$).

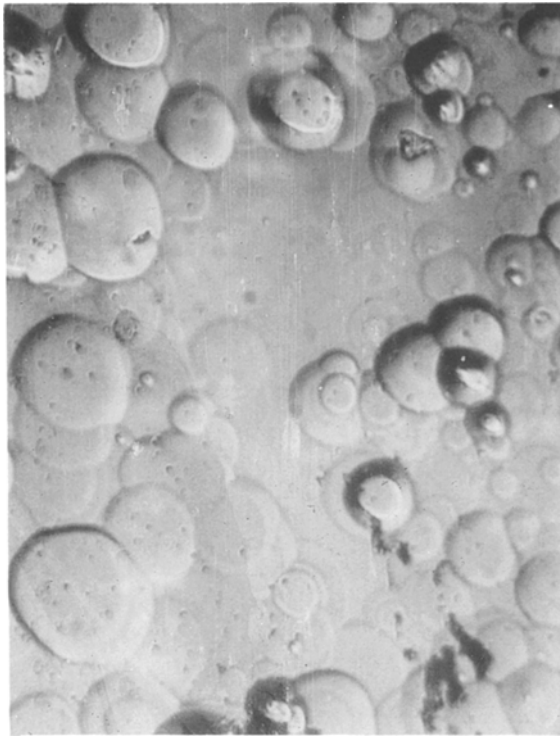


Figure 17 An optical micrograph of a (100) face showing flat- and pointed-topped circular hillocks ($\times 63$).

deposition of LaBO_3 took place during the final stage of growth giving rise to such structures on the habit face of the host LaBO_3 crystal. It was confirmed by EDAX, that the irregular structures in Fig. 18 consisted of LaBO_3 .

All the observations reported here indicate independent growth on LaBO_3 crystal faces by a two-dimensional nucleation mechanism, there being no

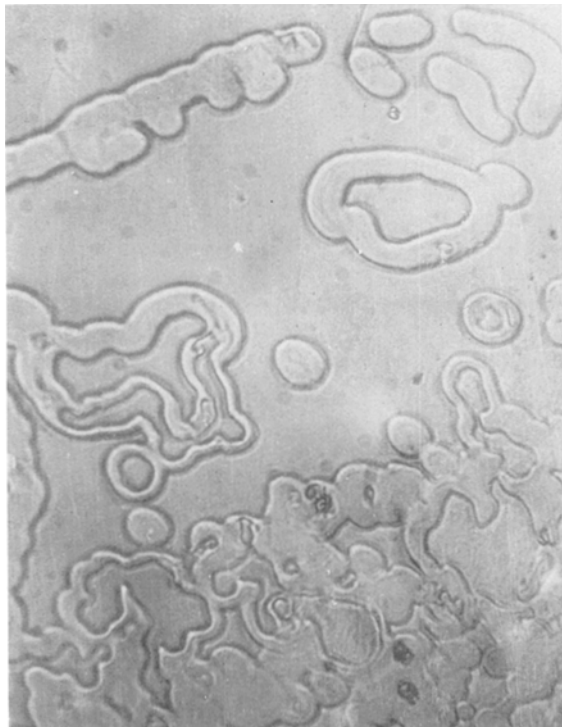


Figure 18 An optical micrograph showing irregular deposition of LaBO_3 on the general host surface ($\times 250$).

evidence to suggest formation of the growth structures observed here by a spiral growth mechanism.

4. Conclusions

1. Surface structures on the habit faces of LaBO_3 crystals include irregularly shaped cavities, structures due to impurity phases, elliptical etch pits, elliptical hillocks, circular hillocks, microcrystals and irregular structures due to thin deposition of LaBO_3 . The observations suggest independent growth of the habit faces of LaBO_3 during the final stages of crystal growth; the independent growth taking place by a two-dimensional nucleation mechanism.

2. The density of dislocations at the sites of elliptical hillocks is much higher than elsewhere on the surface, suggesting such regions to be more imperfect in comparison with others.

3. The impurity phases precipitated in the flux growth of LaBO_3 from the $\text{PbO-B}_2\text{O}_3$ flux system are rich in lead. The impurity phases are deposited on the crystal faces and render them imperfect.

Acknowledgements

We thank Dr G. Garton, Head of the Crystal Growth Group, University of Oxford, for his encouragement in the collaborative research programme. Two authors (A. J. and A. K. R.) thank the University authorities for the award of scholarship and fellowship. The help rendered by Mr V. G. Shah of the Physical Research Laboratory, Ahmedabad, during SEM and EDAX work is acknowledged.

References

1. M. S. JOSHI and A. S. VAGH, *Ind. J. Pure Appl. Phys.* **5** (1967) 318.
2. M. S. JOSHI and P. N. KOTRU, *Jpn. J. Appl. Phys.* **7** (1968) 700.
3. *Idem*, *Amer. Mineral.* **53** (1968) 825.
4. *Idem*, *Kristall und Technik* **11** (1976) 913.
5. *Idem*, *ibid.* **12** (1977) 13.
6. M. S. JOSHI, P. N. KOTRU and A. S. VAGH, *J. Crystal Growth* **2** (1968) 329.
7. *Idem*, *Kristall und Technik* **15** (1980) 1003.
8. M. S. JOSHI and R. K. TAKU, *Ind. J. Pure Appl. Phys.* **10** (1962) 34.
9. K. SANGWAL and A. R. PATEL, *J. Crystal Growth* **23** (1974) 282.
10. P. N. KOTRU, *Jpn. J. Appl. Phys.* **12** (1973) 790.
11. *Idem*, *Kristall und Technik* **13** (1978) 35.
12. P. N. KOTRU and K. K. RAINA, *ibid.* **17** (1982) 1077.
13. K. KIJIMA, N. MIYAMATO and J. NISHIZAWA, *J. Appl. Phys.* **42** (1971) 486.
14. Airtron Report, NONR 4616(00) ARPA 306-62 (1965).
15. R. C. LINARES, NONR 4660 (00) ARPA 306-72 (1965).
16. B. M. WANKLYN, *J. Mater. Sci. Lett.* **8** (1973) 1055.
17. P. N. KOTRU and B. M. WANKLYN, *ibid.* **14** (1979) 755.
18. B. M. WANKLYN, "Practical Aspects of flux growth by spontaneous nucleation", Vol. 1, "Crystal Growth" edited by B. R. Pamplin (Pergamon, Oxford, New York, 1974).
19. E. M. LEVIN, R. S. ROTH and J. B. MARTIN, *Amer. Mineral.* **46** (1961) 1030.
20. R. W. G. WYCKOFF, "Crystal structures" (Wiley, New York, 1964).
21. V. M. GOLDSCHMIDT and H. HAUPTMANN, *Nachr. Ges. Wiss., Göttingen, Math-Phys. Kl.* **53** (1932).
22. B. M. WANKLYN, *J. Crystal Growth* **37** (1977) 334.
23. P. N. KOTRU, S. K. KACHROO and B. M. WANKLYN, *J. Mater. Sci. Lett.* **4** (1985) 1273.

24. *Idem*, *J. Mater. Sci.* **21** (1986) 1609.
25. *Idem*, *ibid.* **21** (1986) 3625.
26. P. N. KOTRU, S. K. KACHROO, B. M. WANKLYN and B. E. WATTS, *ibid.* **22** (1987) 4484.
27. ASHOK K. RAZDAN, S. K. KACHROO, B. L. GUPTA and B. M. WANKLYN, II International Symposium E.MSI, Department of Biophysics, Panjab University, Chandigarh, 31 January to 3 February (1986) Ab-EM-40.
28. P. N. KOTRU, ASHOK K. RAZDAN and B. M. WANKLYN, *J. Mater. Sci.*, in press.

*Received 8 February
and accepted 13 June 1988*